Quench Propagation in 1-D and 2-D Models of High Current Superconductors

Giovanni Volpini
Istituto Nazionale di Fisica Nucleare, Milan, LASA lab.
Via f.lli Cervi 201, 20090 Segrate (MI) Italy, giovanni.volpini@mi.infn.it

Abstract: The understanding of quench, or the sudden transition to the normal state of a high-current superconductor (SC), is fundamental for the design of a SC magnet, and it is widely discussed in the literature.

This paper presents some simple COMSOL™ models, which are compared with well-known approximate formulae and some experimental results. These models allow a more precise description than it is usually done by means of the analytical expressions, and may describe more difficult scenarios, like those involving magnetic diffusion.

Keywords: Type II Superconductors, Quench propagation, Superstabilized conductor, Minimum Propagating Zone

1. Introduction

A typical high current superconducting wire can transport current density in the range of 100 - 1000 A/mm², but this is not a stable condition from a thermodynamic point of view: a small rise of the temperature in a limited section may force it in the normal state. The high Joule dissipation that takes place heats the nearby zones, creating a normal zone which becomes larger and larger, until it eventually encompasses the whole superconductor.

In a real magnet, this temperature rise could be generated by a tiny energy release, like that produced by a wire movement under the effect of the Lorentz forces.

The understanding of this avalanche phenomenon, known as *quench*, is fundamental for the design of a SC magnet, and it has been widely discussed in the literature since the beginning of the practical exploitation of the SC.

This paper presents two fairly simple models, which describe the quench in different conditions, and namely:

1-D model. Here we describe the quench as governed by the longitudinal (i.e. along the wire axis) thermal diffusion only.

2-D model. The cross section of some wire is large enough, and its resistance low enough, that a description of the magnetic diffusion, also in the normal direction (i.e. transversally w.r.t. the wire axis), must be included.

Each of these models is appropriate for different classes of high-current superconductors.

2. 1-D Model

2.1 Governing Equations

In this case, the quench propagation is determined essentially by the longitudinal thermal diffusion (Eq. 1). The superconducting dynamics is introduced by Eq. 2 which describes the current flowing without losses inside the SC filaments *(I_{SC});* the current in excess is carried by the resistive matrix, giving origin to heating through Joule dissipation. Symbols used throughout this paper are explained in the Appendix.

$$\rho_m C_p \, \partial_t T + \nabla \cdot (-k_{th} \nabla T) = \rho_{el} \frac{\left(I_{op} - I_{SC}\right)^2}{A^2} \quad (1)$$

$$I_{SC} = I_{op} \frac{T - T_g}{T_c - T_g} \quad (2)$$

2.2 Quench propagation traditional approach

A simplified solution of Eq. 1 and Eq- 2 [1, page 204 and ff] gives the following formula for the quench propagation velocity:

$$v_q = \frac{J_{op}}{\rho_m C_p} \sqrt{\frac{\rho_{el} k_{th}}{T_s - T_0}} \quad (3)$$

The quench speed does not depend on the features of the initial normal zone, provide that it has a size larger than a characteristic value, known as Minimum Propagating Zone (MPZ): a normal zone smaller than the MPZ simply decays, and the superconductor returns to the environment temperature. The typical length ℓ of

the MPZ can be estimated through [1, page 76, Eq. 5.2]:

$$\ell = \sqrt{\frac{2k_{th}(T_c - T_0)}{J_{op}{}^2 \rho_{el}}} \qquad (4)$$

2.3 Use of COMSOL™ Multiphysics

Simulations have been performed by means of COMSOL™ 3.5 Convention and Conduction (cc) mode. Standard values for the linear system solver (UMFPACK) have been retained.

Boundary conditions impose a zero heat flux at the left boundary ($x = 0$), and a fixed temperature on the right boundary. The former condition requires that the quench starts at $x = 0$, propagating symmetrically rightward and leftward; the latter imposes that the simulation ends before the normal zone reaches the right boundary.

To start the quench, we need to impose an hot spot at $x = 0$, described in §2.4.

The simulation was performed on a 1 m long wire.

2.4 Superconducting wire properties, simulation conditions and results

We simulate a quench propagation on a typical NbTi superconducting wire operated at 4.22 K in an external background field of 5 T, a most standard scenario for accelerator magnets. Its properties are listed in Table 1.

Table 1: Salient features of the superconducting wire used in the 1-D simulations.

Wire diameter	0.8	mm
NbTi volume fraction	0.40	
Critical current @ 4.2 K, 5 T	500	A
Operating current	400	A
Average density	7790	kg/m³
Copper RRR	100	

We used our routine library routine to compute the material properties of the copper and NbTi constituting the wire in the temperature range 4 K – 300 K. We trigger the quench imposing as initial condition an hot spot centered at $x = 0$, having a peak temperature of 8 K, and a guassian shape with a r.m.s. of 5 mm. Fig. 1 shows the normal zone propagation during the quench, moving steadily rightward, while the temperature continues to rise in the quenched section, as a result of the Joule heating.

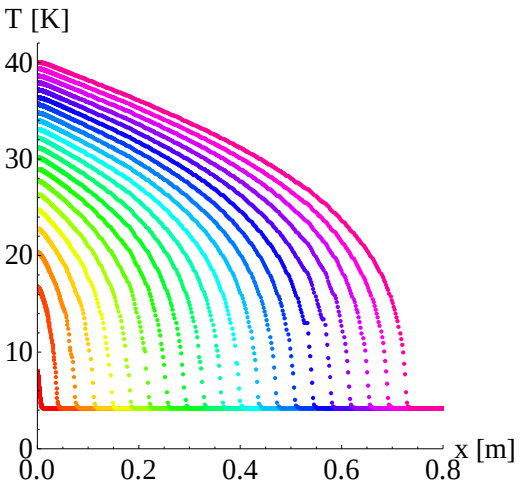

Figure 1. The normal zone propagation during a quench. Temperature profiles along the conductor are computed every 0.001 s. They are shown in red to violet, passing from $t = 0$ s to $t = 0.02$ s.

The abscissa of the arbitrary temperature of 8 K of each quenched profile is shown, as a function of time, in Fig. 2, which demonstrates that the quench moves steadily with a speed of 36.4 m/s. This result is in excellent agreement with the value predicted by Eq. 3, 32 m/s, considering the approximate nature of Eq. 3.

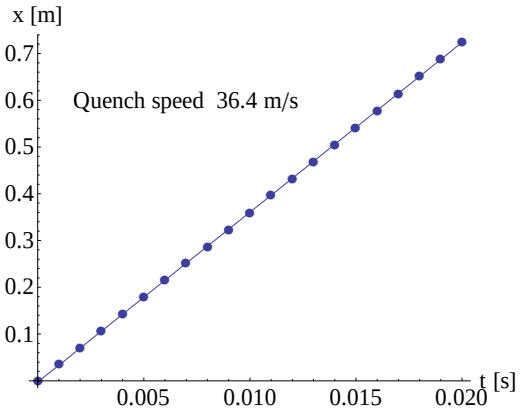

Figure 2. Quench front position from Fig. 1, as a function of time.

We have estimated the size of the MPZ performing simulations with a progressively

smaller initial normal zone, until the quench does not develop any more and the temperature returns to the environmental value, as it is shown in Fig. 3, where the Gaussian r.m.s. of the initial normal zone was fixed at 0.623470 mm. This somewhat artificial value has been chosen because it is only slightly smaller than the MPZ: when the initial normal zone r.m.s. is increased to 0.623475 mm a quench develops and the normal zone propagates at the same speed as in Fig. 1, where the initial normal zone is about ten times larger.

The MPZ total length computed through Eq. 4 is 1.7 mm, or about 3 times the r.m.s. value found here: also in this case the agreement is extremely good.

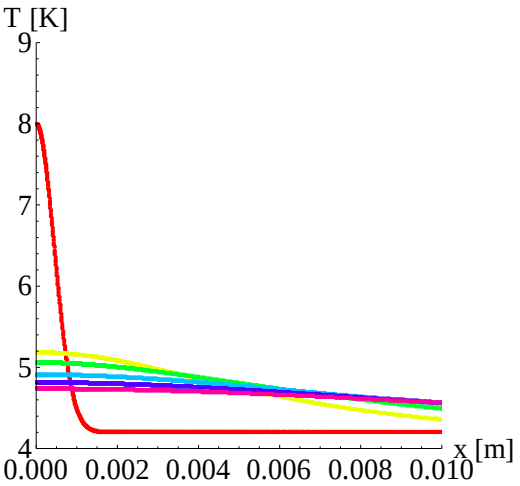

Figure 3. A quench does not develop if the initial normal zone is smaller than the MPZ. Temperature profiles along the conductor are computed every 0.002 s.

3. 2-D Model

3.1 Superconducting Al-stabilized cables

Large (25 m) superconducting magnets, like those used in the particle detectors, exploit cables made of many (10-40) single wires, each similar to that of the 1-D case, twisted and compacted to form the so called *Rutherford cable.* The Rutherford cable is clad by a high purity aluminium matrix, whose purpose is to stabilize and protect the superconductor in case of a quench.

As an example, the conductor of the ATLAS Superconducting Toroidal Magnet at the LHC (CERN) is shown in Fig. 4.

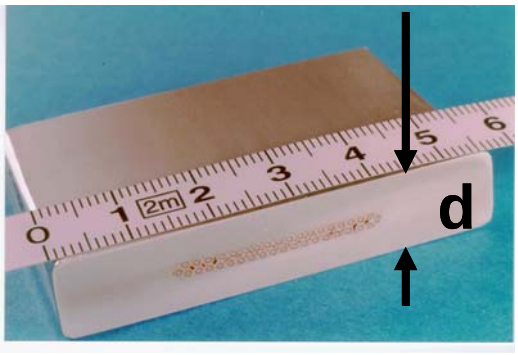

Figure 4. A transverse section of the ATLAS conductor. The NbTi, 40 strand, superconducting Rutherford cable is visible at the centre, surrounded by a high-purity Al matrix.

In order to describe the quench in such cables, it is crucial to appreciate the role of the transverse (w.r.t. the cable axis) magnetic and thermal diffusion time constants, τ_m and τ_m , whose values are respectively:

$$\tau_m = \frac{d^2}{\pi^2 D_m} = \frac{d^2 \mu_0}{\pi^2 \rho_{el}} \approx 0.3\ s$$

$$\tau_\vartheta = \frac{d^2}{\pi^2 D_\vartheta} = \frac{d^2 \rho_m C_p}{\pi^2 k_{th}} \approx 4 \times 10^{-5}\ s \quad .$$

Knowing that the normal zone propagation speed is, for this kind of conductor, of the order of 10 m/s (see §3.5), we see that:

$$\tau_m >> \frac{d}{v_q} \approx 10^{-3}\ s$$

$$\tau_\vartheta << \frac{d}{v_q} \approx 10^{-3}\ s$$

which indicate that while the transverse thermal diffusion is almost instantaneous w.r.t the normal zone propagation, the magnetic diffusion is much slower. The latter fact implies that a proper 2-D description of the magnetic diffusion is mandatory for the Al-stabilized conductors.

In our case, for sake of simplicity, we use 2-D geometries for both the magnetic and the thermal cases, even if a more efficient and elegant solution in COMSOL™ would probably

be constituted by a magnetic 2-D model coupled to a 1-D thermal model.

3.2 Geometrical Model

A 2-D approximation of the cable geometry is used, as described in Fig. 5. The system is assumed to be symmetric with respect to the *x*-*y* plane. The matrix cross-section ABCD has an area equal to half of the conductor matrix section: in this way we can think of the conductor as a section of a infinite system along the *z* direction. In this way, we regard the system as invariant along *z*, and we can consider a 2-D model including only the *x* and *y* space coordinates. We also assume a symmetry across the *x*-*z* plane. The geometrical model used in COMSOL™ is therefore the rectangle BDEF whose length along *x* has been, quite arbitrarily, fixed to 4 m.

The Rutherford cable itself is not part of the geometry, and the superconductor's properties are introduced as a proper boundary condition on side CD.

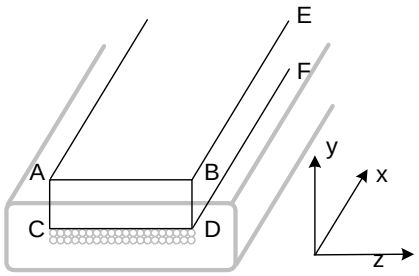

Figure 5. Geometrical model of the cable used in the 2-D simulations. The current flows along the *x*-direction.

3.3 Governing Equations

Here we must introduce explicitly the current, along with the heat, diffusion.

Since the geometry is 2-D, with *x*-*y* coordinates, the ∂_z's are zero for symmetry and the B_x and B_y components of $\vec{B}$ can be set equal to zero. Therefore $\vec{B} = B_z \vec{k}$.

We have now Eq. 5 for the heat diffusion, where the source (right) term describes the Joule dissipation; the current is related to the magnetic induction $\vec{B}$ through Ampère's law (Eq. 6). Magnetic diffusion is described by Eq. 7. The superconductor dynamics is introduced by Eq. 8, similarly to what was done for the 1-D model with Eq. 2.

$$\rho_m C_p \, \partial_t T + \nabla \cdot (-k_{th} \nabla T) = \rho_{el} \left(\frac{1}{\mu_0} \nabla \times B_z \vec{k} \right)^2 \quad (5)$$

$$\vec{J} = \frac{1}{\mu_0} \nabla \times B_z \vec{k} \quad (6)$$

$$\partial_t B_z + \nabla \cdot (-\frac{\rho_{el}}{\mu_0} \nabla B_z) = 0 \quad (7)$$

$$I_{SC} = I_{op} \frac{T - T_g}{T_c - T_g} \quad (8)$$

As it can be seen, this is an intrinsically "multiphysics" problem, since the *T* and *B* variables are coupled in the heat diffusion equation.

3.4 Boundary conditions

Thermal insulation boundary conditions for the thermal equation (Eq. 5) are applied to all the four sides, since the heat source and diffusion are limited within the superconductor. For symmetry reasons, no heat flow takes place also across the BD side, provided that the initial normal zone is symmetric w.r.t. $x = 0$.

Eq. 6 provides the boundary condition for the magnetic induction equation (Eq. 7). Considering the remarks made in §3.3 Eq. 6 becomes:

$$J_x = \frac{1}{\mu_0}(\partial_y B_z - \partial_z B_y) = \frac{1}{\mu_0} \partial_y B_z$$

$$J_y = \frac{1}{\mu_0}(\partial_z B_x - \partial_x B_z) = -\frac{1}{\mu_0} \partial_x B_z$$

and when integrated between 0 and y, it gives the following expression:

$$I_x(x,y) = \int_0^y J_x(x,u)\, du = \frac{1}{\mu_0}(B_z(y) - B_z(0)) \cdot$$

From this, keeping into account the current which is flowing inside the superconducting

Rutherford cable, it is possible to write the B.C.'s on the rectangle's sides, namely:

$$BE \rightarrow \quad B_z = \frac{I_{op}}{\mu_0}$$

$$EF \rightarrow \quad B_z = \frac{I_{op}}{\mu_0}$$

$$DF \rightarrow \quad B_z = \frac{I_{SC}}{\mu_0}$$

$$BD \rightarrow \quad \partial_x B_z = 0$$

The second equation holds only if all the current flows into the superconductor, i.e. only if the normal zone is still far from the right end. The last equation comes from the condition $J_y = 0$ at $x = 0$.

3.5 Simulation conditions and results.

In the simulations, we have assumed the characteristics of the conductor of the End Cap Toroid of the ATLAS detector at LHC, CERN. Its salient features are described in Table 2. The RRR includes the effect of the magnetoresistance, assuming its average effect between 1.2 T and 3 T for a zero-field RRR value of about 1,300.

Table 2: Salient features of the superconducting cable used in the 2-D simulations.

Conductor size	41 x 12	mm²
Rutherford cable critical current @ 4.2 K, 5 T	58,000	A
Aluminium RRR, including magnetoresistance	450	—
Operating temperature	4.8	K

Simulations between 24 kA and 10 kA were performed, in order to compare the results with those reported by [2].

The details of the conditions are reported in Table 3. The intensity of the magnetic field has been computed scaling properly the value quoted by [2, page 1549]. Critical temperature and critical currents have been computed using the formulae reported by [3] and [4], assuming the nominal critical current from Table 2.

Quench was triggered imposing, as initial condition, a gaussian-shaped hot spot region, centered at $x = 0$, whose r.m.s was 0.2 m and having a peak temperature of 9.8 K (or 5 K higher than the environment). In the case of the 10 kA simulation, it was necessary to increase the r.m.s. of the initial normal zone up to 0.40 m, to exceed the MPZ.

Table 3: Simulation parameter list and results

Simulation current [A]	Magnetic field on the conductor [T]	Critical Temperature [K]	Rutherford Cable Critical Current [A]	Quench speed [m/s]
10,000	1.208	8.740	137,663	2.9
15,000	1.813	8.503	110,056	8.6
20,000	2.417	8.262	91,367	16.6
24,000	2.9	8.065	79,741	25.0

As an example, temperature profiles for the simulation at 20 kA, computed every 0.01 s, are shown in Fig. 6.

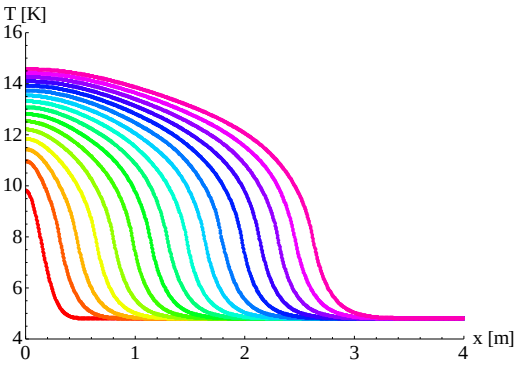

Figure 6. Temperature profiles, computed every 0.01 s from $t = 0$ s until $t = 0.15$ s, for the simulation at 20 kA.

It is apparent that, after a short initial transient, the normal zone front moves steadily. The computed velocities are reported in Table 3 and are also shown in Fig. 7, along with the experimental results [2, Fig. 5].

The agreement is quite good, and it could even be improved if we introduced the heat capacity of the Rutherford cable, which would increase by about 25% the overall thermal capacity, lowering accordingly the quench velocity. Nonetheless we should be extremely cautious about the accuracy of these simulations, keeping in mind that they depend on a rather

larger number of factors, often not precisely known, and that a parametric study of the influence of their uncertainties on the results has not been done, nor it was in the scope of this work.

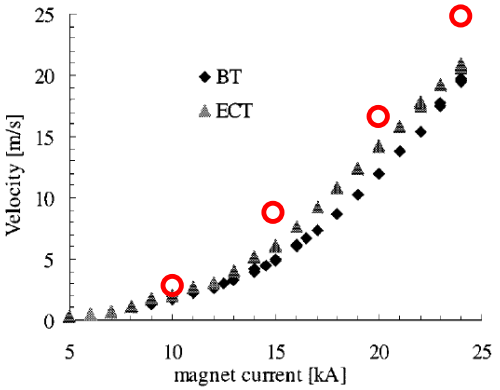

Figure 7. Quench propagation speed measured on the ECT conductor by [2] (triangles), superimposed to the results of our simulations (red rings).

A detail of the current and temperature distribution close to $x = 0$ at $t = 0.1$ s is shown in Fig. 8. We notice that the temperature is constant along the y direction, while the current has not yet redistributed homogenously, as it was explained in § 3.1.

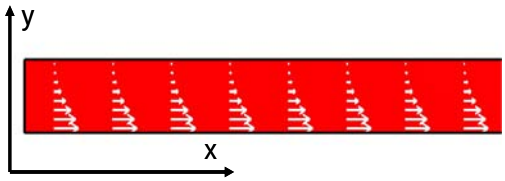

Figure 8. Current (represented by white arrows, whose length is proportional to the module of the current) distribution in the conductor, between $x = 0$ m and $x = 0.05$ m, after 0.1 s, for the simulation at 20 kA shown in Fig. 6. The current has not yet distributed homogeneously transversally (i.e. along the y axis). On the contrary, the temperature is constant to less than 10 mK.

4. Conclusions

The results of quench numerical simulations performed with COMSOL™ are compared with well known analytical approximate expressions for the 1-D case and with some experimental results for the 2-D case. The use of COMSOL™ models gives a better insight of the phenomenon, and it allows to simulate more complex cases where the simpler analytical formulae are not applicable. After suitable adaption, these models could be used to simulate the quench in scenarios with, e.g., thermal exchange on the superconductor's surface or broader superconductor to normal transition curves.

5. References

1. M. N. Wilson, *Superconducting Magnets*. Clarendon Press, Oxford (1983)
2. E. W. Boxman, A. V. Dudarev, and H. H. J. ten Kate, The Normal Zone Propagation in ATLAS B00 Model Coil, *IEEE Trans. on App. Sup.*, **12**, 1549-1552 (2002)
3. M. S. Lubell, Empirical Scaling Formulas for Critical Current and Critical Field for Commercial NbTi, *IEEE Trans. on Mag.*, **19** (3), 754-757 (1983)
4. L. Bottura, A Practical Fit for the Critical Surface of NbTi, *IEEE Trans. on App. Sup.*, **10** (1) 1054-1057 (2000)

6. Acknowledgements

The useful discussions with the ATLAS Magnet Team colleagues on the quench propagation are kindly acknowledged.

7. Appendix

Table 4: List of symbols used in the paper.

ρ_m	mass density
ρ_{el}	electrical resistivity
k_{th}	thermal conductivity
C_p	Specific heat
I_{SC}	current flowing in the superconducting regions only
I_{op}	total (external) current in the SC wire
T_c	superconductor's critical temperature
T_g	generation temperature (when the current begins to flow into the resistive matrix, starting the heating by Joule dissipation)
T_s	$= (T_c + T_s)/2$
A	Superconductor cross-section area
d	Superconductor height (see Fig. 4)
v_q	Normal zone propagation speed